


REVIEW

Open Access



Upper ocean response to tropical cyclones: a review

Han Zhang^{1,2,3*} , Hailun He^{1,2*}, Wen-Zhou Zhang³ and Di Tian¹

Abstract

Tropical cyclones (TCs) are strong natural hazards that are important for local and global air–sea interactions. This manuscript briefly reviews the knowledge about the upper ocean responses to TCs, including the current, surface wave, temperature, salinity and biological responses. TCs usually cause upper ocean near-inertial currents, increase strong surface waves, cool the surface ocean, warm subsurface ocean, increase sea surface salinity and decrease subsurface salinity, causing plankton blooms. The upper ocean response to TCs is controlled by TC-induced mixing, advection and surface flux, which usually bias to the right (left) side of the TC track in the Northern (Southern) Hemisphere. The upper ocean response usually recovers in several days to several weeks. The characteristics of the upper ocean response mainly depend on the TC parameters (e.g. TC intensity, translation speed and size) and environmental parameters (e.g. ocean stratification and eddies). In recent decades, our knowledge of the upper ocean response to TCs has improved because of the development of observation methods and numerical models. More processes of the upper ocean response to TCs can be studied by researchers in the future.

Keywords: Tropical cyclone, Upper ocean, Dynamic response, Temperature and salinity variation, Marine biology

Introduction

Tropical cyclones (TCs) are strong natural hazards that are generated and developed in the ocean. TC wind as well as the TC-induced currents and waves usually damages offshore platforms and vessels, erode coastlines, threaten coastal areas and causes economic and personnel losses (Keim et al. 2007; Wang and Oey 2008; Han et al. 2012; Sun et al. 2013; Zhang et al. 2016b; Li et al. 2018). In recent decades, TC track forecasts have steadily improved because of the development of numerical models (Krishnamurti et al. 1999; McAdie and Lawrence 2000; Bender et al. 2007; Cangialosi and Franklin 2013; Ruf et al. 2016; Montgomery and Smith 2017), while the forecast skill of TC intensity has improved slightly (Cangialosi and Franklin 2013), partly because of inadequate observations and modelling of TC inner cores (Ruf et al.

2016) and TC–ocean interactions (Yano and Emanuel 1991; Montgomery and Smith 2014, 2017). Sea surface temperature is important for TC intensity. For example, a simple coupled model of an axisymmetric hurricane model and one-dimensional ocean model can significantly improve the intensity predictions if the negative feedback of the sea surface temperature to TCs is taken into account (Emanuel 1999). Sea surface temperature cooling greater than 2.5 °C is considered not conducive to TC strengthening (Emanuel 1999) and may even weaken TCs (Schade and Emanuel 1999; Lin et al. 2008). The sea surface cooling caused by a pre-existing TC alters the track and intensity of a subsequent TC (Baranowski et al. 2014; Wu and Li 2018). Note that salinity stratification can reduce sea surface cooling in favour of TC rapid intensification, and this effect increases significantly as the TC intensification rate increases (Balaguru et al. 2020).

TC is also important for the ocean environment, TCs import kinetic energy into surface waves, surface currents and gravitational potential energy, which contributes to ocean diapycnal diffusivity and ocean circulation

*Correspondence: zhanghan@sio.org.cn; hehailun@sio.org.cn

¹ State Key Laboratory of Satellite Ocean Environment Dynamics, Second Institute of Oceanography, Ministry of Natural Resources, Hangzhou 310012, China

Full list of author information is available at the end of the article

(Liu et al. 2008). TCs can also change the local ocean heat uptake (Emanuel 2001) and contribute to global ocean heat transport (D'Asaro et al. 2007; Srivier and Huber 2007; Korty et al. 2008; Pasquero and Emanuel 2008; Hu and Meehl 2009; Fedorov et al. 2010). Some research even considers TCs is important to maintain the permanent El Niño in the early Pliocene epoch (Fedorov et al. 2010). In addition to meridional heat transport, TCs can influence west wind bursts (Lian et al. 2018, 2019), enhance eastward-propagating oceanic Kelvin waves in the tropical Pacific (Wang et al. 2019b) and modulate the occurrence and development of the El Niño–Southern Oscillation. TCs usually cause plankton blooms, which contribute to local long-term primary productivity (Mooers 1975; Foltz et al. 2015). Research shows that TCs increase 20–30% of the primary productivity in the South China Sea every year on average (Lin et al. 2003b; Tang et al. 2004a, b; Sun et al. 2010) also explains 22% of the interannual variability in seasonally averaged (June–November) chlorophyll concentration in the western subtropical North Atlantic (Foltz et al. 2015).

In brief, understanding the ocean response to a TC not only increases the TC forecast skill but also enriches our knowledge of local and global variation of ocean environment.

Ocean response to a tropical cyclone

Current response

The strong TC wind stress arouses upper ocean current response, which usually biases to the right (left) side of TC track in Northern (Southern) Hemisphere, because of better wind-current resonance (Price 1981, 1983; Price et al. 1994; Sun et al. 2015; Zhang et al. 2020b). The wind-current resonance is controlled by non-dimensional TC translation speed which is the ratio of local inertial period to the TC residence time (Zhang et al. 2020b). Generally, a TC causes internal wake in its lee when it moves faster than the first baroclinic wave speed, and the main response is almost centred under the TC and the wake is relatively inconspicuous when a TC moves slower than the speed of first baroclinic wave (Geisler 1970). The current response is a stable Ekman response with surface (bottom) cyclonic divergence (convergence) when TC is stationary (Lu and Huang 2010), and there was weak current response in the lee of the Ekman-like divergence when TC moves slowly (Zhang et al. 2020b). Because the translation speed of most TCs is greater than the local first baroclinic wave speed (e.g. Zhang et al. 2020b), we usually find a near-inertial current response after the TC passage (Pollard 1970; Maeda et al. 1996; Firing et al. 1997; Jarosz et al. 2007; Xu et al. 2019). The upper ocean near-inertial current response to a TC can be divided into mixed layer current and thermocline current (Price 1981;

Price et al. 1994; Zhang et al. 2016a, 2019). TC wind directly drives the mixed layer current, then the divergence and convergence of mixed layer current caused hydrostatic pressure anomaly that drives the thermocline current (Price et al. 1994). The phases of the mixed layer current and thermocline current are nearly uniform within themselves, while there is an angle between mixed layer current and thermocline current (Sanford et al. 2007, 2011; Prakash and Pant 2016; Zhang et al. 2016a), which depends on the ratio of TC translation speed to baroclinic wave speed (Geisler 1970). There is a transition layer between the mixed layer current and thermocline current, with the current phase turning clockwise as the depth increases (Price et al. 1986; Sanford et al. 2011; Zhang et al. 2016a). Velocity shear in transition layer is considered as the primary mechanism for deepening of upper ocean mixed layer during a TC (Glenn et al. 2016; Seroka et al. 2017; Yang et al. 2019). The TC-induced near-inertial current corresponds to upwelling and downwelling, with the transition of the upwelling (downwelling) branch to the downwelling (upwelling) branch being slow and moderate (quick and intense) (Greatbatch 1983, 1984, 1985). If the inertial period signal is removed, there is net mixed layer divergence and upwelling in the right rear quadrant of the TC, as well as net downwelling around the net upwelling zone (Zhang et al. 2018a, b). Relative to open ocean, the current response to a TC in the marginal sea is more complicated because of the secondary local circulation due to the shallow ocean bottom and coastal wall (Halliwell et al. 2011; Glenn et al. 2016; Seroka et al. 2016). TCs also have import positive vorticity into ocean, which intensifies ocean cyclonic eddies (Walker et al. 2005) and alters the three-dimensional structure of eddies (Sun et al. 2014; Lu et al. 2016) or even generates new cyclonic eddies (Chen and Tang 2012; Sun et al. 2014). On the other hand, the circulation of eddies also modulates the TC-induced convection and vertical advection in upper ocean (Jaimes and Shay 2015; Liu et al. 2017).

After TC passage, the current response decays through dispersion and propagation of near-inertial waves (Gill 1984; Park et al. 2009) with an e -folding time from days to weeks (Chen et al. 2013; Yang and Hou 2014). The decay of current is not monotonous because different orders of near-inertial baroclinic waves occasionally resonate again and re-intensify the mixed layer current (Gill 1984). Note that the current velocity to the right side of the TC track decays faster than that to the left side in the Northern Hemisphere (Zhang et al. 2016a; Wu et al. 2020a). The dispersion of waves also results in the tilting of isophasal lines of near-inertial current (Gill 1984; Zhang et al. 2016a). In general, the near-inertial waves propagate in the ocean with a vertical scale of approximately

100–300 m (Kundu 1976; Yang and Hou 2014; Alford et al. 2016) and contribute to turbulent mixing (Qi et al. 1995; Zhai et al. 2009; Jochum et al. 2013). The TC-induced current response can reach the ocean bottom, which may be a major driver of sediment dynamics of continental shelves worldwide (Larcombe and Carter 2004; Galewsky et al. 2006; Dail et al. 2007; Liu et al. 2012), impacting benthic and pelagic habitats by changing water column turbidity or modifying seabed physical characteristics (Hearn and Holloway 1990; Drost et al. 2017). The near-inertial current caused by TCs usually has a blueshift of 1–20% relative to the local inertial frequency, along with slow downward propagation of energy and upward propagation of phase (Pollard 1980; Smith 1989; Yang and Hou 2014). In addition to near-inertial waves, TCs cause inertial waves at a frequency that is two times and three times the local inertial frequency, resulting in energy cascade and dissipation (Niwa and Hibiya 1997; Meroni et al. 2017). Mesoscale ocean processes alter local relative vorticity, which changes the effective planetary vorticity; then, TC-induced near-inertial waves propagate downward more easily in an anticyclonic eddy (Zhai et al. 2005; Guan et al. 2014) and tend to be trapped in a region with more negative vorticity than its surroundings (Oey et al. 2008; Jaimes and Shay 2010) (Fig. 1).

Surface wave response

TC wind also arouses strong surface waves. Sea surface wave height is a function of radial distance from the TC centre by empirical relationships (Young 1988; Wang et al. 2005; Young and Vinoth 2013) and can reach more than 10 m (Zhang et al. 2016a; Drost et al. 2017; Zhang et al. 2018a, b). Surface wave propagation is complicated, and multiple-wave systems are frequently observed. Previous studies typically assumed that TCs impact a region more than 10 times the radius of the maximum wind (Young 2006; Beeden et al. 2015; Esquivel-Trava et al. 2015). TC-induced wave spectra rapidly evolve and vary spatially by radius away from the centre and quadrant of the TC (Moon et al. 2003; Young 2003; Fan et al. 2009; Collins et al. 2018). The TC-induced wave spectra are often bimodal, sometimes trimodal, directional wave spectra (Wright et al. 2001), the waves are asymmetrical, and the directional spectra possess unique characteristics in each quadrant (Hu and Chen 2011; Esquivel-Trava et al. 2015). In reference to the TC heading, single-wave systems propagating towards the left and left-front are usually observed in the front half of the TC coverage area, and multiple-wave systems are generally observed in the back and right quarters outside the radius of maximum wind, while the directional differences and locations of

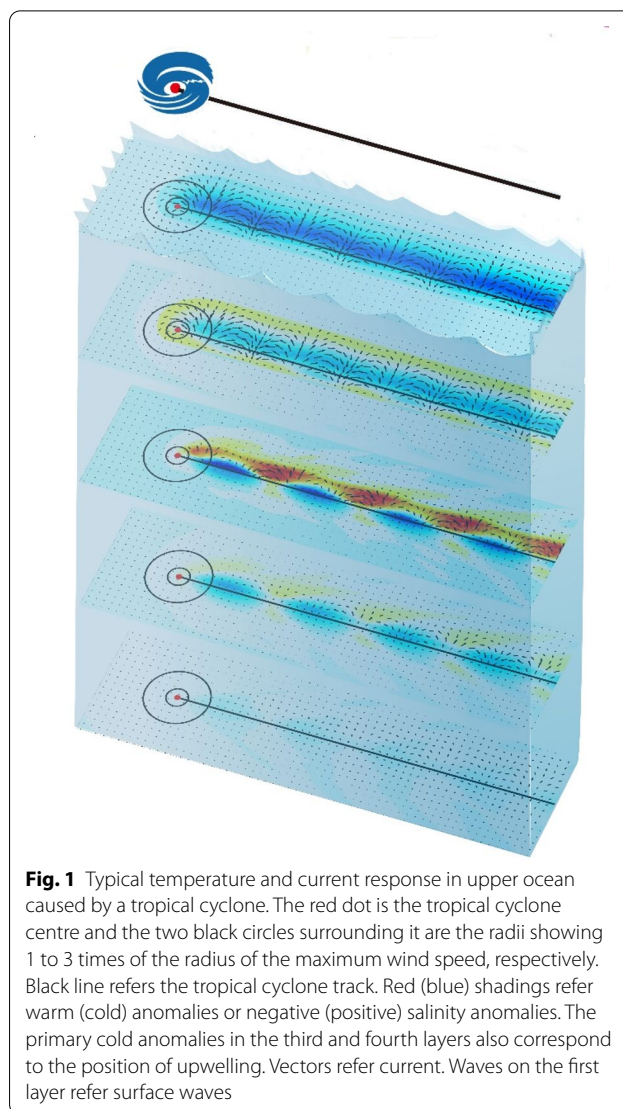


Fig. 1 Typical temperature and current response in upper ocean caused by a tropical cyclone. The red dot is the tropical cyclone centre and the two black circles surrounding it are the radii showing 1 to 3 times of the radius of the maximum wind speed, respectively. Black line refers the tropical cyclone track. Red (blue) shadings refer warm (cold) anomalies or negative (positive) salinity anomalies. The primary cold anomalies in the third and fourth layers also correspond to the position of upwelling. Vectors refer current. Waves on the first layer refer surface waves

multisystem spectra are Gaussian distributions (Hwang and Walsh 2018).

There is misalignment of wind and surface waves during a TC (Fan et al. 2009; Wang et al. 2019a). Swells dominate the surface waves at the front of and outside the central typhoon region (Xu et al. 2017b), and the wave field is more asymmetric than the corresponding TC wind field, mainly due to the “extended fetch”, which exists to the right of a translating TC in the Northern Hemisphere (Young 2003). TC-induced surface currents can reduce the fetch and inhibit the growth of surface waves (Wu et al. 2020b). Nonlinear wave–wave interactions efficiently transfer wave energy from high frequencies to low frequencies and prevent double-peak structures occurring in the frequency-based spectrum (Xu et al. 2017b).

TC-induced surface waves modulate the air–sea surface conditions and fluxes. TC-induced surface waves increase sea surface roughness (Donelan 2004; Makin 2005; Soloviev et al. 2014; Li et al. 2016; Tian et al. 2020) and reduce wind speeds (Olabarrieta et al. 2012). The wind-wave coupling deepens inflow layer, enhances boundary inflow outside the radius of maximum wind and increases the TC intensity (Lee and Chen 2012). Surface wave breaking during TCs also causes a large number of sea spray droplets (Zhang et al. 2011, 2012) in whitecaps and whipping spumes from the tips of waves, which is believed to significantly influence momentum transfer and contributes to the drag coefficient levelling off (or decreasing) at high wind speeds during a TC (Powell et al. 2003; Donelan 2004; Soloviev et al. 2014; Zhang and Song, 2018). Sea spray also influences the air–sea heat flux (Andreas and Mahrt 2016; He et al. 2018; Sun et al. 2019). The latent and sensible heat transfer coefficients are constant at low wind speeds and increase sharply when wind speed at the height of 10 m is greater than 35 m/s (Komori et al. 2018). The air–sea gas transfer also increased significantly due to the surface wave breaking (Iwano et al. 2013; Krall and Jähne 2014; Liang et al. 2020).

TC-induced breaking and unbreaking surface waves also contribute to turbulence in the upper ocean and deepening of the mixed layer (He and Chen, 2011; Toffoli et al. 2012; Aijaz et al. 2017; Stoney et al. 2017; Zhang et al. 2018a, b). The wave-breaking-induced acceleration transfers momentum from surface waves to surface currents and also contributes to sediment transport (Prakash and Pant; 2020). Non-breaking surface wave-induced mixing in numerical model improves the simulations of sea surface temperature and TC track (Guan and Zhao 2014; Li et al. 2014; Aijaz et al. 2017; Stoney et al. 2017). The Craik-Leibovich vortex force, which is the interaction between Stokes drift of surface waves and Eulerian current vorticity, causes Langmuir turbulence (Craik and Leibovich 1976), enhances turbulence entrainment and deepens mixed layer during a TC (Sullivan et al. 2012; Rabe et al. 2015; Reichl et al. 2016a,b; Zhang et al. 2018b; Wang et al. 2018, 2019). The Langmuir cell is roughly aligned with wind and Langmuir turbulence intensity is reduced by wind-wave misalignments during a TC (Wang et al. 2019a, b). Recent researches indicate that parameterization of Langmuir turbulence can improve the simulation of upper ocean temperature and current response during a TC (e.g. Sullivan et al. 2012; Reichl et al. 2016a,b; Blair et al. 2017). The Coriolis–Stokes force also increases the cold upwelling in a slow moving TC and modulates the horizontal advection of upper ocean cold wake (Reichl et al. 2016a; Zhang et al. 2018b). Langmuir circulation generates high-frequency internal waves, induces near-inertial currents at the mixed layer

bottom (the transition layer) and transports more near-inertial energy into deeper layers (e.g. Polton et al. 2008)

Temperature and salinity response

TC deepens the upper ocean mixed layer, cools the sea surface and warms the subsurface (Price 1981, 1983, 1994; Jacob et al. 2000; Zedler et al. 2009; Sanford et al. 2011; Yang et al. 2015; Chen et al., 2020), which is called the “heat pump” effect (Srifer and Huber 2007; Zhang et al. 2016a). Sea surface also lose heat through air–sea heat flux, but it is not as important as the mixing effect for the sea surface cooling (Price 1981; Zhang et al. 2016a). Sea surface cooling usually biased to the right (left) side of the TC track in the Northern (Southern) Hemisphere, and the amplitude of sea surface cooling is usually 1–6 °C (Price 1981; Zedler et al. 2002; Lin et al. 2003a; Black et al. 2007; D’Asaro et al. 2007), sometimes even reaching ~11 °C, resulting in reverse of air–sea surface sensible and latent heat flux (Glenn et al. 2016). The upwelling branch of the near-inertial pumping weakens the subsurface warm anomaly or even turns it to cold anomaly, while downwelling branch intensifies the subsurface warm anomaly. Subsurface warm anomaly caused by mixing can reach as much as ~4 °C, and usually be modulated by the TC-induced near-inertial pumping (Zhang et al. 2016a, 2019). After removing inertial period signal, TC caused a net upwelling with a net cooling in the right rear quadrant of TC, and net downwelling with net warming around the net cooling zone (Zhang et al. 2018a, 2019), which is called “cold suction” effect. During the TC relaxation stage, the air–sea heat flux dominates the upper ocean thermal response, which mainly recovers the sea surface cold anomaly through solar radiation (Price et al. 1986). Research shows that sea surface temperature usually recovers back to its original value in several days to several weeks (Hazelworth 1968; Price et al. 1986, 2008; Emanuel 2001; Hart et al. 2007; Wang et al. 2016), with an e-folding time of approximately one week (Jansen et al. 2010; Dare and McBride 2011), occasionally cooling again during recovery (Price et al. 2008). Subsurface ocean has no contact with air, so it usually recovers slower than the sea surface (Emanuel 2001; Wang et al. 2016).

The characteristics of the upper ocean temperature response to a TC are affected by the TC intensity, size and translation speed (Anthes and Chang 1978; Emanuel et al. 2004; Zhu and Zhang 2006; Samson et al. 2009; Wang et al. 2016; Lin et al. 2017). For example, a stronger TC produces more cooling up to Category 2, but TCs in Categories 3–5 produce less or approximately equal cooling (Lloyd and Vecchi 2011). Argo float observations show that the subsurface warm anomaly is comparable to the near-surface cold anomaly during strong TCs

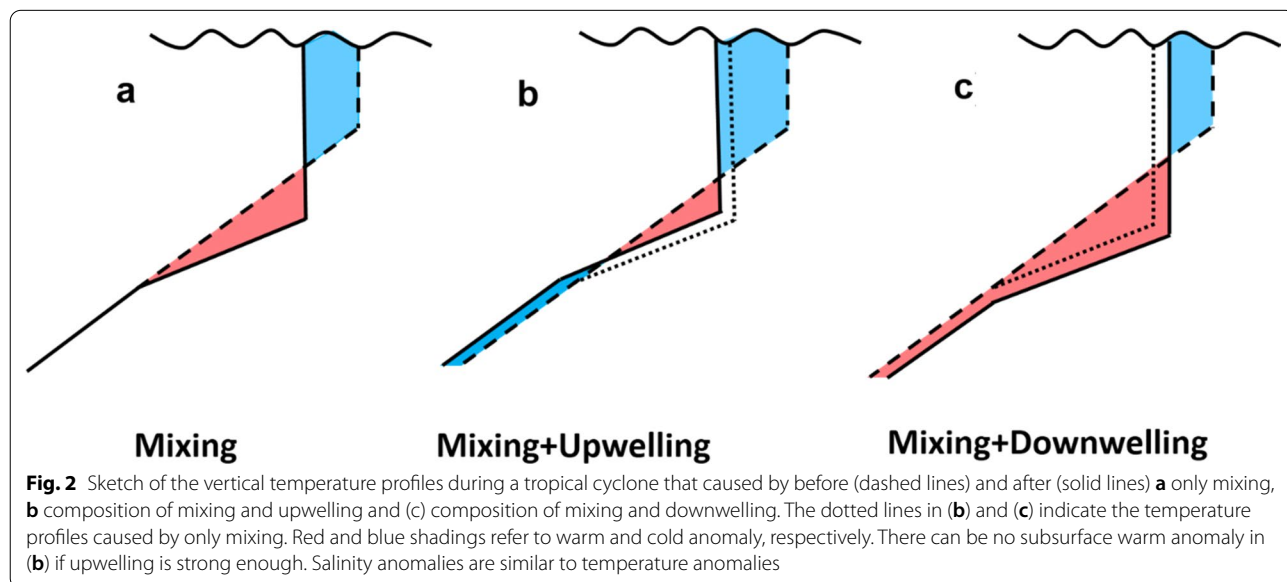
(\geq Category 4), while subsurface warming is not detectable and near-surface cooling is still significant during weak TCs (\leq Category 3), indicating that air–sea heat exchange and upwelling seem to play a somewhat greater role during weak TCs (Park et al. 2011). The sea surface cooling is quasi-symmetric for slow-moving (< 6 m/s) TCs and becomes asymmetric for fast-moving TCs (Samson et al. 2009). The background ocean condition also contributes to the upper ocean temperature response during a TC. For example, there is cold upwelling (warm downwelling) in the core of an anticyclonic (cyclonic) eddy, which intensifies (weakens) sea surface cooling (Jaimes and Shay 2009; Liu et al. 2017; Wu and Li 2018; Ning et al. 2019).

Similar to temperature response, TCs usually increase sea surface salinity and decrease subsurface salinity both within 1 psu, which bias to the right (left) side of TC track in Northern (Southern) Hemisphere (Bond et al. 2011; Girishkumar et al. 2014; Domingues et al. 2015; Zhang et al. 2016a; Abernathy and Haller 2018); the positive sea surface salinity sometimes even reaches 1.5–3 psu (Chaudhuri et al. 2019). However, TC precipitation usually weakens positive sea surface salinity anomaly (Girishkumar et al. 2014; Liu et al. 2020) and causes negative sea surface salinity anomaly to the left (right) side of TC track in the Northern (Southern) Hemisphere (Grodsky et al. 2012; Liu et al. 2014). The freshness of the sea surface by precipitation increases the upper ocean stratification and weakens the TC-induced mixing (Jourdain et al. 2013; Vissa et al. 2013; Liu et al. 2015, 2020), which restricts the sea surface cooling and the negative TC–ocean feedback (Balaguru et al. 2016). There is a barrier layer if the upper ocean isosaline layer is shallower than

the isothermal layer, which also prohibits the deepening of the upper ocean mixed layer caused by a TC (Balaguru et al. 2012; Liu et al. 2015; Yan et al. 2017). Research shows that the upper ocean salinity response can persist about 10–12 days (Girishkumar et al. 2014). The background ocean condition (e.g. eddies) also contributes to the upper ocean salinity response during a TC. For example, the upwelling (downwelling) due to anticyclonic (cyclonic) eddies increases (decreases) upper ocean salinity (Jaimes and Shay 2009; Liu et al. 2017) (Fig. 2).

Biological response

TCs induce phytoplankton blooms and primary production increase, which is mainly attributed to the increased nutrient supply in the euphotic zone induced by vertical mixing (or entrainment) and upwelling during a TC (Mooers 1975; Morimoto et al. 2009; Siswanto et al. 2009; Zheng et al. 2010; Chiang et al. 2011; Shibano et al. 2011; Hung et al. 2013; Huang and Oey 2015) and ocean restratification after the TC (Huang and Oey 2015; Lin and Oey 2016). The chlorophyll increases after a TC usually ranges from 5 to 91% (Babin et al. 2004; Zhao et al. 2017; Xu et al. 2017a), while a lingered slow-moving TC (Kai-Tak in year 2000) can even triggered 30-fold of surface chlorophyll-a concentration (Lin et al. 2003b). In Northern (Southern) Hemisphere, the chlorophyll increases usually biases to the right (left) side of the TC track (Lin et al. 2003b; Babin et al. 2004; Yin et al. 2007; Hanshaw et al. 2008; Shang et al. 2008; Zhao et al. 2008; Zheng et al. 2010; Shibano et al. 2011), although the rightward (leftward) bias is not obvious or may even occur towards the left (right) side of the TC track (Zheng et al. 2010; Shibano et al. 2011). The amplitude and scope of surface



plankton blooms depend not only on the TC characteristics but also on the ocean background conditions (Lin et al. 2003b; Zhao et al. 2008; Chen and Tang 2012; Shang et al. 2015; Xu et al. 2017a). For example, weak and slow-moving TCs induce phytoplankton blooms with higher chlorophyll-a concentrations, while strong and fast-moving TCs induce blooms over a larger area (Zhao et al. 2008). A pre-existing cold core eddy plays an important role in the increase in chlorophyll-a concentration by TCs (Chen and Tang 2012; Shang et al. 2015; Xu et al. 2017a; Jin et al. 2020), and the concentration of pre-existing chlorophyll-a in cold core eddies is approximately 25–45% (8–25%) of that of the post-existing chlorophyll-a in cold core eddies for relatively high (low) TC transition speeds (Shang et al. 2015). The biological response in coastal regions is more complicated than that in the open ocean (Pan et al. 2017). TC-induced mixing, enhanced terrestrial runoff and resuspension are considered three major processes that contribute to the increased nutrient concentrations and subsequent primary production in the euphotic layer (Chen et al. 2003). The chlorophyll-a reaches its peak three days after nitrate peak after a TC (Pan et al. 2017), and TC-induced phytoplankton blooms usually last for two to three weeks (Babin et al. 2004; Chen and Tang 2012; Foltz et al. 2015; Wang 2020).

Discussion and conclusions

This work reviews the upper ocean response to tropical cyclones, including the current, surface wave, temperature, salinity and biological responses. TC usually causes

upper ocean near-inertial currents, increases strong surface waves, cools (warms) the surface (subsurface) ocean and increases (decreases) surface (subsurface) salinity, also causing plankton blooms. The upper ocean response is controlled by mixing, advection and air–sea flux (i.e. heat flux and fresh water flux). The upper ocean response usually biases to the right (left) side of the TC track because the wind–current resonance is stronger (weaker) and the corresponding mixing is stronger (weaker) on the right (left) side in the Northern (Southern) Hemisphere. The characteristics of the upper ocean response mainly depend on the TC parameters (e.g. TC intensity, translation speed and size) and environmental parameters (e.g. ocean stratification and eddies) (Fig. 3).

In recent decades, the understanding of upper ocean response to a tropical cyclone has improved because of the development of observations and modelling. Traditional observation methods such as buoys and moorings (Black and Dickey 2008; Zhang et al. 2016a, 2019; Yang et al. 2019), air-deployed drifters and floats (Black et al. 2007; D’Asaro et al. 2007; Pun et al. 2011; Sanford et al. 2011), Argo floats (Park et al. 2011; Vissa et al. 2012; Wu and Chen 2012; Fu et al. 2014; Liu et al. 2014; Lin et al., 2017; Chen et al., 2020) and satellite remote sensing (Li et al. 2018; Yue et al. 2018; Ning et al. 2019; Zhang et al. 2019), as well as new observation technology and methods such as gliders (Domingues et al. 2015; Miles et al. 2015; Hsu and Ho 2018) and wave gliders (Mitarai and McWilliams 2016), are now applied to TC–ocean observations. Regarding numerical model simulations, early

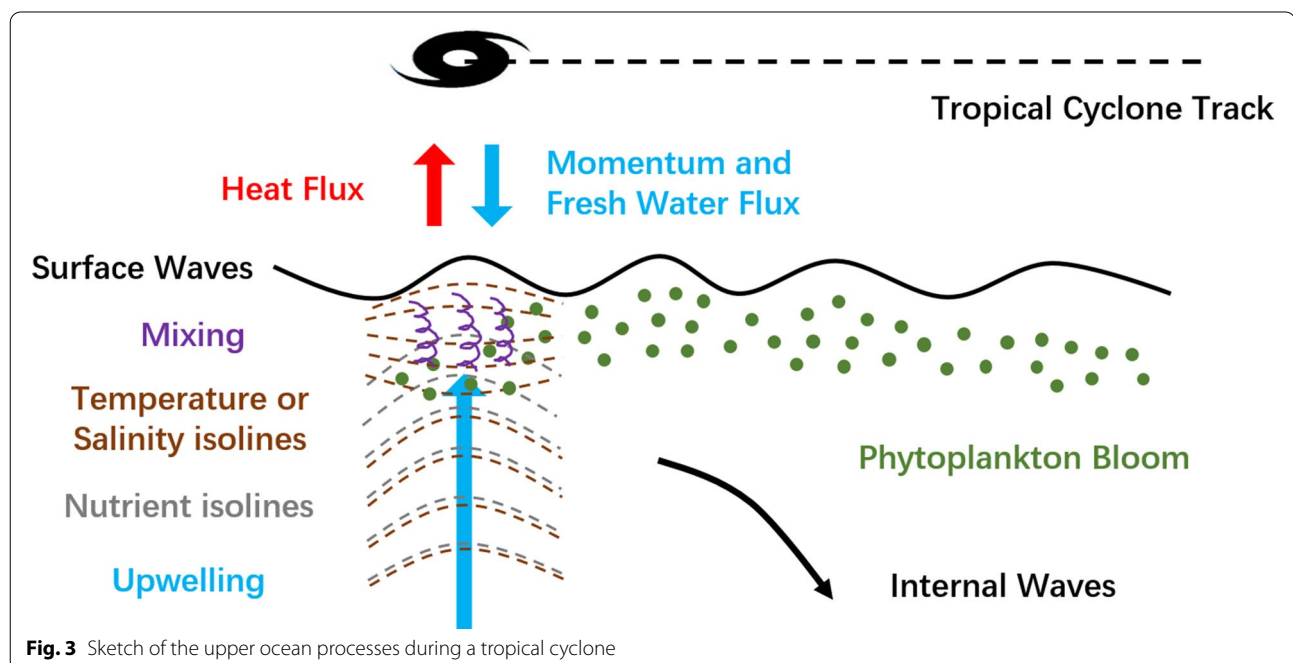


Fig. 3 Sketch of the upper ocean processes during a tropical cyclone

works use the slab ocean model to reproduce the ocean current response (Geisler 1970; Pollard and Millard 1970; Gill 1984), followed by several numerical models such as the three-dimensional Price–Weller–Pinkel model (3DPWP) (Price et al. 1994; Sanford et al. 2007; Guan et al. 2014; Zhang et al. 2016a), the regional oceanic modelling system (ROMS) (Yue et al. 2018) and the Massachusetts Institute of Technology Ocean General Circulation Model (MIT OGCM) (Zedler et al. 2009) to reproduce the three-dimensional current, temperature and salinity responses. Wave models such as the Simulating WAVes Nearshore (SWAN) (Liu et al. 2007; Huang et al. 2013) and WAVEWATCH-III (Moon et al. 2003; Xu et al. 2017b; Qiao et al. 2019) models are used to reproduce the sea surface wave response to a TC. Recently, atmosphere–ocean–wave models such as the Coupled Ocean–Atmosphere–Wave–Sediment Transport (COAWST) modelling system (Prakash and Pant 2016; Wu et al. 2018) have been gradually applied to simulate the ocean response to TCs. Note that the ocean ecological model seems to have not been widely used for the simulation of ocean biological response to a TC yet. What is more, new technology such as big data and machine learning provide a new way to study TC–ocean interaction (e.g. Wei et al. 2017, 2018; Jiang et al. 2018).

Although our understanding of the upper ocean response to a TC has increased in recent decades, some fields merit further study, such as: 1. the characteristics of the air–sea interface as well as the surface flux during TCs; 2. the effect of varied TCs on the upper ocean response, e.g. the upper ocean response during curved TC track, during intensifying (weakening) TCs or accelerating (decelerating) TCs; 3. the interaction between TCs and mesoscale or submesoscale eddies; 4. the upper ocean response to sequential TCs; 5. the effects of TCs on large ocean circulation, e.g. modulation of global ocean circulation by the kinetic energy and heat uptake caused by TCs; 6. the processes that control the recovery of the upper ocean response after TCs; and 7. the propagation of TC-induced anomalies into the ocean interior and deep ocean.

Some existing issues in observation, numerical model and technology restrict the study of upper ocean response to TCs. In situ observation of air–sea interface (i.e. air–sea flux, surface waves) and deep ocean is in shortage, which restricts our understanding of the air–sea interaction and how upper ocean anomalies propagate into ocean interior. The coupling of atmospheric and oceanic model as well as the parameterization of the processes in air–sea interface merits further study for better simulation of TC–ocean interaction. What is more, it is a common problem that surface currents simulated by model seems stronger and persists longer as well as less vertical

propagation of current signals than observation (Huang et al. 2009; Sanford et al. 2011; Zedler et al. 2009; Zhang et al. 2016a, b). In general, accurate prediction of tropical cyclone and oceanic conditions requires proper initialization of both atmospheric and oceanic components of the modelling system, as well as accurate measurements of the ocean ahead of the TC, and skillful assimilation of the ocean data into the ocean model. Besides, the practicability of the usage of big data and machine learning for the study of the upper ocean response to a TC still needs further exploration. We hope the development of science and technology in the future will uncover more processes and mechanisms of TC–ocean interactions, help improve TC forecasts and enhance our understanding of local and global air–sea interactions.

Acknowledgements

We thank Yuntao Wang and Fei Chai from Second Institute of Oceanography, Ministry of Natural Resources for their helpful suggestions of the improvement of Fig. 3.

Authors' contributions

HZ wrote the whole manuscript and HH, WZ and DT revised the manuscript. All authors read and approved the final manuscript.

Funding

This work was supported by the Scientific Research Fund of the Second Institute of Oceanography, MNR (QNYC2002), the National Key R&D Program of China (2018YFC1506403), the National Programme on Global Change and Air–Sea Interaction (GASI-04-WLHY-01), the Oceanic Interdisciplinary Program of Shanghai Jiao Tong University (SL2020MS032), the National Natural Science Foundation of China (41806021, 41730535, 41705048, 41976007, 41776015), the CEES Visiting Fellowship Program (CEESRS202001) and the State Key Laboratory of Tropical Oceanography, South China Sea Institute of Oceanology, Chinese Academy of Sciences (LTO2007).

Availability of data and materials

Not applicable.

Competing interests

The authors declare that they have no competing interests.

Author details

¹ State Key Laboratory of Satellite Ocean Environment Dynamics, Second Institute of Oceanography, Ministry of Natural Resources, Hangzhou 310012, China. ² Southern Marine Science and Engineering Guangdong Laboratory (Zhuhai), Zhuhai 519082, China. ³ Fujian Provincial Key Laboratory for Coastal Ecology and Environmental Studies, Xiamen University, Xiamen 361102, China.

Received: 3 April 2020 Accepted: 1 December 2020

Published online: 08 January 2021

References

- Abernathey R, Haller G (2018) Transport by lagrangian vortices in the Eastern Pacific. *J Phys Oceanogr* 48:667–685
- Aijaz S, Ghantous M, Babanin AV, Ginis I, Thomas B, Wake G (2017) Nonbreaking wave-induced mixing in upper ocean during tropical cyclones using coupled hurricane–ocean–wave modeling. *J Geophys Res Oceans* 122:3939–3963
- Alford MH, MacKinnon JA, Simmons HL, Nash JD (2016) Near-inertial internal gravity waves in the ocean. *Ann Rev Mar Sci* 8:95–123
- Andreas EL, Mahrt L (2016) On the prospects for observing spray-mediated air–sea transfer in wind–water tunnels. *J Atmos Sci* 73:185–198

- Anthes RA, Chang SW (1978) Response of the hurricane boundary layer to changes of sea surface temperature in a numerical model. *J Atmos Sci* 35:1240–1255
- Babin SM, Carton JA, Dickey TD, Wiggert JD (2004) Satellite evidence of hurricane-induced phytoplankton blooms in an oceanic desert. *J Geophys Res Oceans* 109:C03043
- Balaguru K, Chang P, Saravanan R, Leung LR, Xu Z, Li M, Hsieh JS (2012) Ocean barrier layers' effect on tropical cyclone intensification. *Proc Natl Acad Sci U S A* 109:14343–14347
- Balaguru K, Foltz GR, Leung LR, Emanuel KA (2016) Global warming-induced upper-ocean freshening and the intensification of super typhoons. *Nat Commun* 7:13670
- Balaguru K, Foltz GR, Leung LR, Xu KJ, W, Reul N, Chapron B, (2020) Pronounced impact of salinity on rapidly intensifying tropical cyclones. *Bull Amer Meteor Soc* 101(9):E1497–E1511
- Baranowski D, Flatau P, Chen S, Black P (2014) Upper ocean response to the passage of two sequential typhoons. *Ocean Sci* 10:559–570
- Beeden R, Maynard J, Puotinen M, Marshall P, Dryden J, Goldberg J, Williams G (2015) Impacts and recovery from severe tropical cyclone yasi on the great barrier reef. *PLoS ONE* 10:e0121272
- Bender MA, Ginis I, Tuleya R, Thomas B, Marchok T (2007) The operational GFDL coupled hurricane–ocean prediction system and a summary of its performance. *Mon Weather Rev* 135:3965–3989
- Black PG, D'Asaro EA, Drennan WM, French JR, Niiler PP, Sanford TB, Terrill EJ, Walsh EJ, Zhang JA (2007) Air–sea exchange in hurricanes: synthesis of observations from the coupled boundary layer air–sea transfer experiment. *Bull Am Meteorol Soc* 88:357–374
- Black WJ, Dickey TD (2008) Observations and analyses of upper ocean responses to tropical storms and hurricanes in the vicinity of Bermuda. *J Geophys Res* 113:C08009
- Blair A, Ginis I, Hara T, Ullhorn E (2017) Impact of Langmuir turbulence on upper ocean response to hurricane edouard: model and observations. *J Geophys Res Oceans* 122:9712–9724
- Bond NA, Cronin MF, Sabine C, Kawai Y, Ichikawa H, Freitag P, Ronnholm K (2011) Upper ocean response to Typhoon Choi-Wan as measured by the Kuroshio extension observatory mooring. *J Geophys Res* 116:C02031
- Cangialosi J, Franklin J (2013) 2010 National hurricane center forecast verification report. NOAA/NWS/NCEP/National Hurricane Center, Miami
- Chaudhuri D, Sengupta D, D'Asaro E, Venkatesan R, Ravichandran M (2019) Response of the salinity-stratified Bay of Bengal to cyclone Phailin. *J Phys Oceanogr* 49(5):1121–1140
- Chen SS, Lee CY (2012) Symmetric and asymmetric structures of hurricane boundary layer in coupled atmosphere–wave–ocean models and observations. *J Atmos Sci* 69:3576–3594
- Chen H, Li S, He HL, Song JB, Ling Z, Cao AZ, Zou ZS, Qiao WL (2020) Observational study of super typhoon Meranti (2016) using satellite, surface drifter. *Argo float and reanalysis data*, *Acta Oceanol Sin*
- Chen CTA, Liu CT, Chuang WS, Yang YJ, Shiah FK, Tang TY, Chung SW (2003) Enhanced buoyancy and hence upwelling of subsurface Kuroshio waters after a typhoon in the Southern East China sea. *J Mar Syst* 42:65–79
- Chen Y, Tang D (2012) Eddy-feature phytoplankton bloom induced by a tropical cyclone in the South China sea. *Int J Remote Sens* 33:7444–7457
- Chen G, Xue H, Wang D, Xie Q (2013) Observed near-inertial kinetic energy in the northwestern South China sea. *J Geophys Res Oceans* 118:4965–4977
- Chiang TL, Wu CR, Oey LY (2011) Typhoon kai-tak: an ocean's perfect storm. *J Phys Oceanogr* 41:221–233
- Collins CO, Potter H, Lund B, Tamura H, Graber HC (2018) Directional wave spectra observed during intense tropical cyclones. *J Geophys Res Oceans* 123:773–793
- Craik ADD, Leibovich S (1976) A rational model for Langmuir circulations. *J Fluid Mech* 73:401–426
- D'Asaro EA, Sanford TB, Niiler PP, Terrill EJ (2007) Cold wake of hurricane frances. *Geophys Res Lett* 34:L15609
- Dail MB, Corbett DR, Walsh JP (2007) Assessing the importance of tropical cyclones on continental margin sedimentation in the Mississippi delta region. *Cont Shelf Res* 27:1857–1874
- Dare RA, McBride JL (2011) Sea surface temperature response to tropical cyclones. *Mon Weather Rev* 139:3798–3808
- Domingues R, Goni G, Bringas F, Lee SK, Kim HS, Halliwell G, Dong J, Morell J, Pomales L (2015) Upper ocean response to hurricane gonzalo (2014): salinity effects revealed by targeted and sustained underwater glider observations. *Geophys Res Lett* 42:7131–7138
- Donelan MA (2004) On the limiting aerodynamic roughness of the ocean in very strong winds. *Geophys Res Lett* 31:L18306
- Drost EJJ, Lowe RJ, Ivey GN, Jones NL, Péquignot CA (2017) The effects of tropical cyclone characteristics on the surface wave fields in Australia's North West region. *Cont Shelf Res* 139:35–53
- Emanuel KA (1999) Thermodynamic control of hurricane intensity. *Nature* 401:665–669
- Emanuel K (2001) Contribution of tropical cyclones to meridional heat transport by the oceans. *J Geophys Res Atmos* 106:14771–14781
- Emanuel K, Desautels C, Holloway C, Korty R (2004) Environmental control of tropical cyclone intensity. *J Geophys Res* 61(7):843–858
- Esquivel-Trava B, Ocampo-Torres FJ, Osuna P (2015) Spatial structure of directional wave spectra in hurricanes. *Ocean Dyn* 65:65–76
- Fan Y, Ginis I, Hara T, Wright CW, Walsh EJ (2009) Numerical simulations and observations of surface wave fields under an extreme tropical cyclone. *J Phys Oceanogr* 39:2097–2116
- Fedorov AV, Brierley CM, Emanuel K (2010) Tropical cyclones and permanent El Niño in the early pliocene epoch. *Nature* 463:1066–1070
- Firing E, Lien RC, Muller P (1997) Observations of strong inertial oscillations after the passage of tropical cyclone ofa. *J Geophys Res Oceans* 102:3317–3322
- Foltz GR, Balaguru K, Leung LR (2015) A reassessment of the integrated impact of tropical cyclones on surface chlorophyll in the western subtropical North Atlantic. *Geophys Res Lett* 42:1158–1164
- Fu H, Wang X, Chu PC, Zhang X, Han G, Li W (2014) Tropical cyclone footprint in the ocean mixed layer observed by argo in the Northwest Pacific. *J Geophys Res Oceans* 119:8078–8092
- Galewsky J, Stark CP, Dadson S, Wu CC, Sobel AH, Horng MJ (2006) Tropical cyclone triggering of sediment discharge in Taiwan. *J Geophys Res Earth Surf* 111:F03014
- Geisler JE (1970) Linear theory of the response of a two layer ocean to a moving hurricane. *Geophys Fluid Dyn* 1:249–272
- Gill AE (1984) On the behavior of internal waves in the wakes of storms. *J Phys Oceanogr* 14:1129–1151
- Girishkumar MS, Suprit K, Chiranjivi J, Bhaskar TVSU, Ravichandran M, Shesu RV, Rao EPR (2014) Observed oceanic response to tropical cyclone jal from a moored buoy in the South-Western Bay of Bengal. *Ocean Dyn* 64:325–335
- Glenn SM, Miles TN, Seroka GN, Xu Y, Forney RK, Yu F, Roarty H, Schofield O, Kohut J (2016) Stratified coastal ocean interactions with tropical cyclones. *Nat Commun* 7:10887
- Greatbatch RJ (1983) On the response of the ocean to a moving storm: the nonlinear dynamics. *J Phys Oceanogr* 13:357–367
- Greatbatch RJ (1984) On the response of the ocean to a moving storm: parameters and scales. *J Phys Oceanogr* 14:59–78
- Greatbatch RJ (1985) On the role played by upwelling of water in lowering sea surface temperatures during the passage of a storm. *J Geophys Res* 90:11751
- Grodsky SA, Reul N, Lagerloef G, Reverdin G, Carton JA, Chapron B, Quilfen Y, Kudryavtsev VN, Kao HY (2012) Haline hurricane wake in the Amazon/Orinoco plume: AQUARIUS/SACD and SMOS observations. *Geophys Res Lett* 39(20):L20603
- Guan S, Zhao W, Huhtnance J, Tian J, Wang J (2014) Observed upper ocean response to typhoon megi (2010) in the Northern South China sea. *J Geophys Res Oceans* 119:3134–3157
- Halliwell GR, Shay LK, Brewster JK, Teague WJ (2011) Evaluation and sensitivity analysis of an ocean model response to hurricane Ivan. *Mon Weather Rev* 139:921–945
- Han G, Ma Z, Chen D, Deyoung B, Chen N (2012) Observing storm surges from space: hurricane igor off newfoundland. *Sci Rep* 2:1010
- Hanshaw MN, Lozier MS, Palter JB (2008) Integrated impact of tropical cyclones on sea surface chlorophyll in the North Atlantic. *Geophys Res Lett* 35:L01601
- Hart RE, Maue RN, Watson MC (2007) Estimating local memory of tropical cyclones through MPI anomaly evolution. *Mon Weather Rev* 135:3990–4005

- Hazelworth JB (1968) Water temperature variations resulting from hurricanes. *J Geophys Res* 73:5105–5123
- He HL, Chen DK (2011) Effects of surface wave breaking on the oceanic boundary layer. *Geophys Res Lett* 38(7):L07604
- He HL, Wu QY, Chen DK, Sun J, Liang CJ, Jin WF, Xu Y (2018) Effects of surface waves and sea spray on the air-sea fluxes during the passage of Typhoon Hagupit. *Acta Oceanol Sin* 37(5):1–7
- Hearn CJ, Holloway PE (1990) A three-dimensional barotropic model of the response of the Australian North West Shelf to tropical cyclones. *J Phys Oceanogr* 20:60–80
- Hsu PC, Ho CR (2018) Typhoon-induced ocean subsurface variations from glider data in the Kuroshio region adjacent to Taiwan. *J Oceanogr* 75:1–21
- Hu K, Chen Q (2011) Directional spectra of hurricane-generated waves in the Gulf of Mexico. *Geophys Res Lett* 38:L19608
- Hu A, Meehl GA (2009) Effect of the Atlantic hurricanes on the oceanic meridional overturning circulation and heat transport. *Geophys Res Lett* 36:L03702
- Huang SM, Oey LY (2015) Right-side cooling and phytoplankton bloom in the wake of a tropical cyclone. *J Geophys Res Oceans* 120:5735–5748
- Huang PS, Sanford TB, Imberger J (2009) Heat and turbulent kinetic energy budgets for surface layer cooling induced by the passage of Hurricane Frances (2004). *J Geophys Res Oceans* 114:C12023
- Huang Y, Weisberg RH, Zheng L, Zijlema M (2013) Gulf of Mexico hurricane wave simulations using SWAN: bulk formula-based drag coefficient sensitivity for hurricane ike. *J Geophys Res Oceans* 118:3916–3938
- Hung CC, Chung CC, Gong GC, Jan S, Tsai Y, Chen KS, Chou WC, Lee MA, Chang Y, Chen MH, Yang WR, Tseng CJ, Gawarkiewicz G (2013) Nutrient supply in the Southern East China sea after Typhoon Morakot. *J Mar Res* 71:133–149
- Hwang PA, Walsh EJ (2018) Propagation directions of ocean surface waves inside tropical cyclones. *J Phys Oceanogr* 48:1495–1511
- Iwano K, Takagaki N, Kurose R, Komori S (2013) Mass transfer velocity across the breaking air–water interface at extremely high wind speeds. *Tellus B* 65:21341
- Jacob SD, Shay LK, Mariano AJ, Black PG (2000) The 3D oceanic mixed layer response to hurricane Gilbert. *J Phys Oceanogr* 30:1407–1429
- Jaimes B, Shay LK (2009) Mixed layer cooling in mesoscale oceanic eddies during hurricanes Katrina and Rita. *Mon Wea Rev* 137(12):4188–4207
- Jaimes B, Shay LK (2010) Near-inertial wave wake of hurricanes Katrina and Rita over mesoscale oceanic eddies. *J Phys Oceanogr* 40(6):1320–1337
- Jaimes B, Shay LK (2015) Enhanced wind-driven downwelling flow in warm oceanic eddy features during the intensification of tropical cyclone ISAAC (2012): observations and theory. *J Phys Oceanogr* 45(6):1667–1689
- Jansen MF, Ferrari R, Mooring TA (2010) Seasonal versus permanent thermocline warming by tropical cyclones. *Geophys Res Lett* 37:L03602
- Jarosz E, Hallock ZR, Teague WJ (2007) Near-inertial currents in the DeSoto Canyon region. *Cont Shelf Res* 27:2407–2426
- Jiang G, Xu J, Wei J (2018) A deep learning algorithm of neural network for the parameterization of typhoon-ocean feedback in typhoon forecast models. *Geophys Res Lett* 45:3706–3716
- Jin W, Liang C, Hu J, Meng Q, Lü H, Wang Y, Lin F, Chen X, Liu X (2020) Modulation effect of mesoscale eddies on sequential typhoon-induced oceanic responses in the South China Sea. *Remote Sens* 12:3059
- Jochum M, Briegleb BP, Danabasoglu G, Large WG, Norton NJ, Jayne SR, Alford MH, Bryan FO (2013) The impact of oceanic near-inertial waves on climate. *J Clim* 26:2833–2844
- Jourdain NC, Lengaigne M, Vialard J, Madec G, Menkes CE, Vincent EM, Jullien S, Barnier B (2013) Observation-based estimates of surface cooling inhibition by heavy rainfall under tropical cyclones. *J Phys Oceanogr* 43:205–221
- Keim BD, Muller RA, Stone GW (2007) Spatiotemporal patterns and return periods of tropical storm and hurricane strikes from Texas to Maine. *J Clim* 20:3498–3509
- Krall KE, Jähne B (2014) First laboratory study of air–sea gas exchange at hurricane wind speeds. *Ocean Sci* 10(2):257–265
- Komori S, Takahashi K, Kurose R, Onishi R, Takagaki N, Iwano K, Suzuki N (2018) Laboratory measurements of heat transfer and drag coefficients at extremely high wind speeds. *J Phys Oceanogr* 48:959–974
- Korty RL, Emanuel KA, Scott JR (2008) Tropical cyclone-induced upper-ocean mixing and climate: application to equable climates. *J Clim* 21:638–654
- Krishnamurti TN, Kishtawal CM, LaRow TE, Bacchiocchi DR, Zhang Z, Williford CE, Gadgil S, Surendran S (1999) Improved weather and seasonal climate forecasts from multimodel superensemble. *Science* 285:1548–1550
- Kundu PK (1976) An analysis of inertial oscillations observed near Oregon coast. *J Phys Oceanogr* 6:879–893
- Larcombe P, Carter R (2004) Cyclone pumping, sediment partitioning and the development of the great barrier reef shelf system: a review. *Quat Sci Rev* 23:107–135
- Li X, Han G, Yang J, Chen D, Zheng G, Chen N (2018) Using satellite altimetry to calibrate the simulation of typhoon seth storm surge off Southeast China. *Remote Sens* 10:657
- Li Y, Peng S, Wang J, Yan J (2014) Impacts of nonbreaking wave-stirring-induced mixing on the upper ocean thermal structure and typhoon intensity in the South China Sea. *J Geophys Res Oceans* 119:5052–5070
- Li FN, Song JB, He HL, Li S, Li X, Guan SD (2016) Assessment of surface drag coefficient parameterizations based on observations and simulations using the Weather Research and Forecasting model. *Atmos Oceanic Sci Lett* 9(4):327–336
- Lian T, Chen D, Tang Y, Liu X, Feng J, Zhou L (2018) Linkage between westerly wind bursts and tropical cyclones. *Geophys Res Lett* 45:11431–11438
- Lian T, Ying J, Ren HL, Zhang C, Liu T, Tan XX (2019) Effects of tropical cyclones on ENSO. *J Clim* 32:6423–6443
- Liang J-H, D'Asaro EA, McNeil C, Fan Y, Harcourt RR, Emerson SR, Yang B, Sullivan PP (2020) Suppression of CO₂ outgassing by gas bubbles under a hurricane. *Geophys Res Lett* 47:20
- Lin H, Liu WT, Wu C-C, Chiang JCH, Sui C-H (2003a) Satellite observations of modulation of surface winds by typhoon-induced upper ocean cooling. *Geophys Res Lett* 30(3):1131
- Lin H, Liu WT, Wu C-C, Wong GTF, Hu C, Chen Z, Liang W-D, Yang Y, Liu K-K (2003b) New evidence for enhanced ocean primary production triggered by tropical cyclone. *Geophys Res Lett* 30:1718
- Lin YC, Oey LY (2016) Rainfall-enhanced blooming in typhoon wakes. *Sci Rep* 6:31310
- Lin H, Wu C-C, Pun I-F, Ko D-S (2008) Upper-ocean thermal structure and the Western North Pacific category 5 typhoons. Part I: ocean features and the category 5 typhoons' intensification. *Mon Weather Rev* 136:3288–3306
- Lin S, Zhang W-Z, Shang S-P, Hong H-S (2017) Ocean response to typhoons in the western North Pacific: composite results from Argo data. *Deep-Sea Res, Part I* 123:62–74
- Liu JC, Liou YA, Wu MX, Lee YJ, Cheng CH, Kuei CP, Hong RM (2015) Analysis of interactions among two tropical depressions and typhoons tembin and bolaven (2012) in Pacific ocean by using satellite cloud images. *IEEE Trans Geosci Remote Sens* 53:1394–1402
- Liu SS, Sun L, Wu Q, Yang YJ (2017) The responses of cyclonic and anticyclonic eddies to typhoon forcing: the vertical temperature-salinity structure changes associated with the horizontal convergence/divergence. *J Geophys Res Oceans* 122:4974–4989
- Liu LL, Wang W, Huang RX (2008) The mechanical energy input to the ocean induced by tropical cyclones. *J Phys Oceanogr* 38:1253–1266
- Liu JT, Wang YH, Yang RJ, Hsu RT, Kao SJ, Lin HL, Kuo FH (2012) Cyclone-induced hyperpycnal turbidity currents in a submarine canyon. *J Geophys Res Oceans* 117:C04033
- Liu H, Xie L, Pietrafesa LJ, Bao S (2007) Sensitivity of wind waves to hurricane wind characteristics. *Ocean Model* 18:37–52
- Liu Z, Xu J, Sun C, Wu X (2014) An upper ocean response to typhoon bolaven analyzed with argo profiling floats. *Acta Oceanol Sin* 33:90–101
- Liu F, Zhang H, Ming J, Zheng J, Tian D, Chen D (2020) Importance of precipitation on the upper ocean salinity response to typhoon kalmaegi (2014). *Water* 12:614
- Lloyd ID, Vecchi GA (2011) Observational evidence for oceanic controls on hurricane intensity. *J Clim* 24:1138–1153
- Lu ZM, Huang RX (2010) The three-dimensional steady circulation in a homogeneous ocean induced by a stationary hurricane. *J Phys Oceanogr* 40:1441–1457
- Lu Z, Wang G, Shang X (2016) Response of a preexisting cyclonic ocean eddy to a typhoon. *J Phys Oceanogr* 46:2403–2410

- Maeda A, Uejima K, Yamashiro T, Sakurai M, Ichikawa H, Chaen M, Taira K, Mizuno S (1996) Near inertial motion excited by wind change in a margin of the typhoon 9019. *J Oceanogr* 52:375–388
- Makin VK (2005) A note on the drag of the sea surface at hurricane winds. *Bound-Layer Meteorol* 115:169–176
- McAdie CJ, Lawrence MB (2000) Improvements in tropical cyclone track forecasting in the Atlantic basin, 1970–98. *Bull Am Meteorol Soc* 81:989–997
- Meroni AN, Miller MD, Tziperman E, Pasquero C (2017) Nonlinear energy transfer among ocean internal waves in the wake of a moving cyclone. *J Phys Oceanogr* 47:1961–1980
- Miles T, Seroka G, Kohut J, Schofield O, Glenn S (2015) Glider observations and modeling of sediment transport in hurricane sandy. *J Geophys Res Oceans* 120:1771–1791
- Mitarai S, McWilliams JC (2016) Wave glider observations of surface winds and currents in the core of typhoon danas. *Geophys Res Lett* 43(11):312–319
- Montgomery MT, Smith RK (2014) Paradigms for tropical cyclone intensification. *Aust Meteorol Ocean* 64:37–66
- Montgomery MT, Smith RK (2017) Recent developments in the fluid dynamics of tropical cyclones. *Annu Rev Fluid Mech* 49:541–574
- Mooers CNK (1975) Several effects of a baroclinic current on the cross-stream propagation of inertial-internal waves. *Geophys Fluid Dyn* 6:245–275
- Moon IJ, Ginis I, Hara T, Tolman HL, Wright CW, Walsh EJ (2003) Numerical simulation of sea surface directional wave spectra under hurricane wind forcing. *J Phys Oceanogr* 33:1680–1706
- Morimoto A, Kojima S, Jan S, Takahashi D (2009) Movement of the Kuroshio axis to the Northeast shelf of Taiwan during typhoon events. *Estuar Coast Shelf Sci* 82:547–552
- Ning J, Xu Q, Zhang H, Wang T, Fan K (2019) Impact of cyclonic ocean eddies on upper ocean thermodynamic response to typhoon soudelor. *Remote Sens* 11:938
- Niwa Y, Hibiya T (1997) Nonlinear processes of energy transfer from traveling hurricanes to the deep ocean internal wave field. *J Geophys Res Oceans* 102:12469–12477
- Oey LY, Inoue M, Lai R, Lin XH, Welsh SE, Rouse LJ (2008) Stalling of near-inertial waves in a cyclone. *Geophys Res Lett* 35:L12604
- Olabarrieta M, Warner JC, Armstrong B, Zambon JB, He R (2012) Ocean–atmosphere dynamics during hurricane ida and norida: an application of the coupled ocean–atmosphere–wave–sediment transport (COAWST) modeling system. *Ocean Model* 43–44:112–137
- Pan G, Chai F, Tang D, Wang D (2017) Marine phytoplankton biomass responses to typhoon events in the South China Sea based on physical–biogeochemical model. *Ecol Modell* 356:38–47
- Park JJ, Kim K, Schmitt RW (2009) Global distribution of the decay timescale of mixed layer inertial motions observed by satellite-tracked drifters. *J Geophys Res* 114:C11010
- Park JJ, Kwon YO, Price JF (2011) Argo array observation of ocean heat content changes induced by tropical cyclones in the North Pacific. *J Geophys Res* 116:C12025
- Pasquero C, Emanuel K (2008) Tropical cyclones and transient upper-ocean warming. *J Clim* 21:149–162
- Pollard RT (1970) On the generation by winds of inertial waves in the ocean. *Deep Sea Res Oceanogr Abstr* 17:795–812
- Pollard RT (1980) Properties of near-surface inertial oscillations. *J Phys Oceanogr* 10:385–398
- Pollard RT, Millard RC (1970) Comparison between observed and simulated wind-generated inertial oscillations. *Deep Sea Res Oceanogr Abstr* 17:813–821
- Polton JA, Smith JA, Mackinnon JA, Tejada-Martínez AE (2008) Rapid generation of high-frequency internal waves beneath a wind and wave forced oceanic surface mixed layer. *Geophys Res Lett* 35:L13602
- Powell MD, Vickery PJ, Reinhold TA (2003) Reduced drag coefficient for high wind speeds in tropical cyclones. *Nature* 422(279):283
- Prakash KR, Pant V (2016) Upper oceanic response to tropical cyclone phailin in the Bay of Bengal using a coupled atmosphere–ocean model. *Ocean Dyn* 67:51–64
- Prakash KR, Pant V (2020) On the wave–current interaction during the passage of a tropical cyclone in the Bay of Bengal. *Deep-Sea Res Part II* 172:104658
- Price JF (1981) Upper ocean response to a hurricane. *J Phys Oceanogr* 11:153–175
- Price JF (1983) Internal wave wake of a moving storm. Part I. Scales, energy budget and observations. *J Phys Oceanogr* 13:949–965
- Price JF, Morzel J, Niiler PP (2008) Warming of SST in the cool wake of a moving hurricane. *J Geophys Res* 113:C07010
- Price JF, Sanford TB, Forristall GZ (1994) Forced stage response to a moving hurricane. *J Phys Oceanogr* 24:233–260
- Price JF, Weller RA, Pinkel R (1986) Diurnal cycling: observations and models of the upper ocean response to diurnal heating, cooling, and wind mixing. *J Geophys Res* 91:8411
- Pun I, Chang YT, Lin II, Tang TY, Lien RC (2011) Typhoon–ocean interaction in the Western North Pacific: part 2. *Oceanography* 24:32–41
- Qi H, De Szoeke RA, Paulson CA, Eriksen CC (1995) The structure of near-inertial waves during ocean storms. *J Phys Oceanogr* 25:2853–2871
- Qiao W, Song J, He H, Li F (2019) Application of different wind field models and wave boundary layer model to typhoon waves numerical simulation in WAVEWATCH III model. *Tellus A Dyn Meteorol Oceanogr* 71:1657552
- Rabe TJ, Kukulka T, Ginis I, Hara T, Reichl BG, D’Asaro EA, Harcourt RR, Sullivan PP (2015) Langmuir Turbulence under Hurricane Gustav (2008). *J Phys Oceanogr* 45:657–677
- Reichl BG, Ginis I, Hara T, Thomas B, Kukulka T, Wang D (2016a) Impact of Sea-State-Dependent Langmuir Turbulence on the Ocean Response to a Tropical Cyclone. *Mon Wea Rev* 144:4569–4590
- Reichl BG, Wang D, Hara T, Ginis I, Kukulka T (2016b) Langmuir Turbulence Parameterization in Tropical Cyclone Conditions. *J Phys Oceanogr* 46:863–886
- Ruf CS, Atlas R, Chang PS, Clarizia MP, Garrison JL, Gleason S, Katzberg SJ, Jelenak Z, Johnson JT, Majumdar SJ, Obrien A, Posselt DJ, Ridley AJ, Rose RJ, Zavorotny VU (2016) New ocean winds satellite mission to probe hurricanes and tropical convection. *Bull Am Meteorol Soc* 97:385–395
- Samson G, Giordani H, Caniaux G, Roux F (2009) Numerical investigation of an oceanic resonant regime induced by hurricane winds. *Ocean Dyn* 59:565–586
- Sanford TB, Price JF, Girtton JB (2011) Upper-ocean response to hurricane frances (2004) observed by profiling EM-APEX floats. *J Phys Oceanogr* 41:1041–1056
- Sanford TB, Price JF, Girtton JB, Webb DC (2007) Highly resolved observations and simulations of the ocean response to a hurricane. *Geophys Res Lett* 34:L13604
- Schade LR, Emanuel KA (1999) The ocean’s effect on the intensity of tropical cyclones: results from a simple coupled atmosphere–ocean model. *J Atmos Sci* 56:642–651
- Seroka G, Miles T, Xu Y, Kohut J, Schofield O, Glenn S (2016) Hurricane irene sensitivity to stratified coastal ocean cooling. *Mon Weather Rev* 144:3507–3530
- Seroka G, Miles T, Xu Y, Kohut J, Schofield O, Glenn S (2017) Rapid shelf-wide cooling response of a stratified coastal ocean to hurricanes. *J Geophys Res Oceans* 122:4845–4867
- Shang S, Li L, Sun F, Wu J, Hu C, Chen D, Ning X, Qiu Y, Zhang C, Shang S (2008) Changes of temperature and bio-optical properties in the South China sea in response to typhoon lingling, 2001. *Geophys Res Lett* 35:L10602
- Shang XD, Zhu HB, Chen GY, Xu C, Yang Q (2015) Research on cold core eddy change and phytoplankton bloom induced by typhoons: case studies in the South China sea. *Adv Meteorol* 2015:1–19
- Shibano R, Yamanaka Y, Okada N, Chuda T, Suzuki SI, Niino H, Toratani M (2011) Responses of marine ecosystem to typhoon passages in the western subtropical North Pacific. *Geophys Res Lett* 38:L18608
- Siswanto E, Morimoto A, Kojima S (2009) Enhancement of phytoplankton primary productivity in the Southern East China sea following episodic typhoon passage. *Geophys Res Lett* 36:L11603
- Smith PC (1989) Inertial oscillations near the coast of Nova Scotia during CASP. *Atmos–Ocean* 27:181–209
- Soloviev AV, Lukas R, Donelan MA, Haus BK, Ginis I (2014) The air–sea interface and surface stress under tropical cyclones. *Sci Rep* 4:5306
- Sriver RL, Huber M (2007) Observational evidence for an ocean heat pump induced by tropical cyclones. *Nature* 447:577–580
- Stoney L, Walsh K, Babanin AV, Ghantous M, Govekar P, Young I (2017) Simulated ocean response to tropical cyclones: the effect of a novel

- parameterization of mixing from unbroken surface waves. *J Adv Model Earth Syst* 9:759–780
- Sullivan PP, Romero L, McWilliams JC, Melville WK (2012) Transient evolution of Langmuir turbulence in ocean boundary layers driven by hurricane winds and waves. *J Phys Oceanogr* 42:1959–1980
- Sun Y, Chen C, Beardsley RC, Xu Q, Qi J, Lin H (2013) Impact of current-wave interaction on storm surge simulation: a case study for hurricane bob. *J Geophys Res Oceans* 118:2685–2701
- Sun J, He HL, Hu XM, Wang DQ, Gao C, Song JB (2019) Numerical simulations of typhoon Hagupit (2008) using WRF. *Wea Forecasting* 34(4):999–1015
- Sun L, Li YX, Yang YJ, Wu Q, Chen XT, Li QY, Li YB, Xian T (2014) Effects of super typhoons on cyclonic ocean eddies in the Western North Pacific: a satellite data-based evaluation between 2000 and 2008. *J Geophys Res Oceans* 119:5585–5598
- Sun J, Oey L-Y, Chang R, Xu F, Huang S-M (2015) Ocean response to typhoon Nuri (2008) in western Pacific and South China Sea. *Ocean Dyn* 65(5):735–749
- Sun L, Yang Y, Xian T, Lu Z, Fu Y (2010) Strong enhancement of chlorophyll a concentration by a weak typhoon. *Mar Ecol Prog Ser* 404:39–50
- Tang DL, Kawamura H, Van Dien T, Lee MA (2004b) Offshore phytoplankton biomass increase and its oceanographic causes in the South China sea. *Mar Ecol Prog Ser* 268:31–41
- Tang DL, Kawamura H, Doan-Nhu H, Takahashi W (2004a) Remote sensing oceanography of a harmful algal bloom off the coast of Southeastern Vietnam. *J Geophys Res Oceans* 109:C03014
- Tian D, Zhang H, Zhang W, Zhou F, Sun X, Zhou Y, Ke D (2020) Wave glider observations of surface waves during three tropical cyclones in the South China Sea. *Water* 12:1331
- Toffoli A, McConochie J, Ghantous M, Loffredo L, Babanin AV (2012) The effect of wave-induced turbulence on the ocean mixed layer during tropical cyclones: field observations on the Australian North-West shelf. *J Geophys Res Oceans* 117:24
- Vissa NK, Satyanarayana ANV, Kumar BP (2012) Response of upper ocean during passage of MALA cyclone utilizing ARGO data. *Int J Appl Earth Obs Geoinf* 14:149–159
- Vissa NK, Satyanarayana ANV, Kumar BP (2013) Response of upper ocean and impact of barrier layer on sidr cyclone induced sea surface cooling. *Ocean Sci J* 48:279–288
- Walker ND, Leben RR, Balasubramanian S (2005) Hurricane-forced upwelling and chlorophyllaenhancement within cold-core cyclones in the Gulf of Mexico. *Geophys Res Lett* 32:L18610
- Wang Y (2020) Composite of typhoon induced sea surface temperature and chlorophyll-a responses in the South China Sea. *J Geophys Res Oceans* 125:20
- Wang D, Kukulka T, Reichl BG, Hara T, Ginis I (2019a) Wind-wave misalignment effects on Langmuir turbulence in tropical cyclone conditions. *J Phys Oceanogr* 49:3109–3126
- Wang D, Kukulka T, Reichl BG, Hara T, Ginis I, Sullivan PP (2018) Interaction of Langmuir turbulence and inertial currents in the ocean surface boundary layer under tropical cyclones. *J Phys Oceanogr* 48(1921):1940
- Wang Q, Li J, Jin FF, Chan JCL, Wang C, Ding R, Sun C, Zheng F, Feng J, Xie F, Li Y, Li F, Xu Y (2019b) Tropical cyclones act to intensify El Nino. *Nat Commun* 10:3793
- Wang DW, Mitchell DA, Teague WJ, Jarosz E, Hulbert MS (2005) Extreme waves under hurricane ivan. *Science* 309:896
- Wang D, Kukulka T, Reichl BG, Hara T, Ginis I, Sullivan PP (2018) Interaction of Langmuir turbulence and inertial currents in the ocean surface boundary layer under tropical cyclones. *J Phys Oceanogr* 48(9):1921–1940
- Wang DP, Oey LY (2008) Hindcast of waves and currents in hurricane katrina. *Bull Am Meteorol Soc* 89:487–496
- Wang G, Wu L, Johnson NC, Ling Z (2016) Observed three-dimensional structure of ocean cooling induced by Pacific tropical cyclones. *Geophys Res Lett* 43:7632–7638
- Wei J, Jiang G, Liu X (2017) Parameterization of typhoon-induced ocean cooling using temperature equation and machine learning algorithms: an example of typhoon Soulik (2013). *Ocean Dyn* 67:1179–1193
- Wei J, Liu X, Jiang G (2018) Parameterizing sea surface temperature cooling induced by tropical cyclones using a multivariate linear regression model. *Acta Oceanol Sin* 37:1–10
- Wright CW, Walsh EJ, Vandemark D, Krabill WB, Garcia AW, Houston SH, Powell MD, Black PG, Marks FD (2001) Hurricane directional wave spectrum spatial variation in the open ocean. *J Phys Oceanogr* 31:2472–2488
- Wu Q, Chen D (2012) Typhoon-induced variability of the oceanic surface mixed layer observed by argo floats in the Western North Pacific ocean. *Atmos-Ocean* 50:4–14
- Wu Z, Chen J, Jiang C, Liu X, Deng B, Qu K, He Z, Xie Z (2020b) Numerical investigation of Typhoon Kai-tak (1213) using a mesoscale coupled WRF-ROMS model—part II: Wave effects. *Ocean Eng* 196:106805
- Wu R, Li C (2018) Upper ocean response to the passage of two sequential typhoons. *Deep Sea Res I Oceanogr Res Pap* 132:68–79
- Wu R, Zhang H, Chen D (2020a) Effect of typhoon kalmaegi (2014) on Northern South China sea explored using multi-platform satellite and buoy observations data. *Prog Oceanogr* 180:102218
- Wu R, Zhang H, Chen D, Li C, Lin J (2018) Impact of typhoon kalmaegi (2014) on the South China sea: simulations using a fully coupled atmosphere-ocean-wave model. *Ocean Model* 131:132–151
- Xu Y, He H, Song J, Hou Y, Li F (2017b) Observations and modeling of typhoon waves in the South China Sea. *J Phys Oceanogr* 47:1307–1324
- Xu J, Huang Y, Chen Z, Liu J, Liu T, Li J, Cai S, Ning D (2019) Horizontal variations of typhoon-forced near-inertial oscillations in the South China sea simulated by a numerical model. *Cont Shelf Res* 180:24–34
- Xu F, Yao Y, Oey L, Lin Y (2017a) Impacts of pre-existing ocean cyclonic circulation on sea surface chlorophyll-a concentrations off northeastern Taiwan following episodic typhoon passages. *J Geophys Res Oceans* 122:6482–6497
- Yan Y, Li L, Wang C (2017) The effects of oceanic barrier layer on the upper ocean response to tropical cyclones. *J Geophys Res Oceans* 122:4829–4844
- Yang YJ, Chang MH, Hsieh CY, Chang HI, Jan S, Wei CL (2019) The role of enhanced velocity shears in rapid ocean cooling during super typhoon nepartak 2016. *Nat Commun* 10:1627
- Yang B, Hou Y (2014) Near-inertial waves in the wake of 2011 typhoon nesat in the Northern South China sea. *Acta Oceanol Sin* 33:102–111
- Yang B, Hou Y, Hu P, Liu Z, Liu Y (2015) Shallow ocean response to tropical cyclones observed on the continental shelf of the Northwestern South China sea. *J Geophys Res Oceans* 120:3817–3836
- Yano JI, Emanuel K (1991) An Improved Model of the Equatorial Troposphere and Its Coupling with the Stratosphere. *J Atmos* 48(3):377–389
- Yin X, Wang Z, Liu Y, Xu Y (2007) Ocean response to typhoon ketsana traveling over the Northwest Pacific and a numerical model approach. *Geophys Res Lett* 34:L21606
- Young IR (1988) Parametric hurricane wave prediction model. *J Waterw Port Coast Ocean Eng* 114:637–652
- Young IR (2003) A review of the sea state generated by hurricanes. *Mar Struct* 16:201–218
- Young IR (2006) Directional spectra of hurricane wind waves. *J Geophys Res* 111:C08020
- Young IR, Vinoth J (2013) An “extended fetch” model for the spatial distribution of tropical cyclone wind-waves as observed by altimeter. *Ocean Eng* 70:14–24
- Yue X, Zhang B, Liu G, Li X, Zhang H, He Y (2018) Upper ocean response to typhoon kalmaegi and sarika in the South China sea from multiple-satellite observations and numerical simulations. *Remote Sens* 10:348
- Zedler SE, Dickey TD, Doney SC, Price JF, Yu X, Mellor GL (2002) Analyses and simulations of the upper ocean’s response to hurricane felix at the Bermuda testbed mooring site: 13–23 August 1995. *J Geophys Res Oceans* 107:25
- Zedler SE, Niiler PP, Stammer D, Terrill E, Morzel J (2009) Ocean’s response to hurricane frances and its implications for drag coefficient parameterization at high wind speeds. *J Geophys Res* 114:C04016
- Zhai X, Greatbatch RJ, Eden C, Hibiya T (2009) On the loss of wind-induced near-inertial energy to turbulent mixing in the upper ocean. *J Phys Oceanogr* 39:3040–3045
- Zhai X, Greatbatch RJ, Zhao J (2005) Enhanced vertical propagation of storm-induced near-inertial energy in an eddying ocean channel model. *Geophys Res Lett* 32:L18602
- Zhang H, Chen D, Zhou L, Liu X, Ding T, Zhou B (2016a) Upper ocean response to typhoon kalmaegi (2014). *J Geophys Res Oceans* 121:6520–6535
- Zhang X, Chu PC, Li W, Liu C, Zhang L, Shao C, Zhang X, Chao G, Zhao Y (2018) Impact of Langmuir turbulence on the thermal response of the ocean

- surface mixed layer to Supertyphoon Haitang (2005). *J Phys Oceanogr* 48:1651–1674
- Zhang W, Cui Y, Santos A, Hanebuth TJJ (2016) Storm-driven bottom sediment transport on a high-energy narrow shelf (NW Iberia) and development of mud depocenters. *J Geophys Res Oceans* 121:5751–5772
- Zhang X, Han G, Wang D, Deng Z, Li W (2012) Summer surface layer thermal response to surface gravity waves in the yellow sea. *Ocean Dyn* 62:983–1000
- Zhang X, Han G, Wang D, Li W, He Z (2011) Effect of surface wave breaking on the surface boundary layer of temperature in the yellow sea in summer. *Ocean Model* 38:267–279
- Zhang H, Liu X, Wu R, Chen D, Zhang D, Shang X, Wang Y, Song X, Jin W, Yu L, Qi Y, Tian D, Zhang W (2020) Sea surface current response patterns to a tropical cyclones. *J Mar Syst* 12:56
- Zhang H, Liu X, Wu R, Liu F, Yu L, Shang X, Qi Y, Wang Y, Song X, Xie X, Yang C, Tian D, Zhang W (2019) Ocean response to successive typhoons Sarika and Haima (2016) based on data acquired via multiple satellites and moored array. *Remote Sens* 11:2360
- Zhang T, Song JB (2018) Effects of sea surface waves and ocean spray on air-sea momentum fluxes. *Adv Atmos Sci* 35:469–478
- Zhang H, Wu R, Chen D, Liu X, He H, Tang Y, Ke D, Shen Z, Li J, Xie J, Tian D, Ming J, Liu F, Zhang D, Zhang W (2018) Net modulation of upper ocean thermal structure by typhoon kalmaegi (2014). *J Geophys Res Oceans* 123:7154–7171
- Zhang D, Zhang H, Zheng J, Cheng X, Tian D, Chen D (2020a) Changes in tropical-cyclone translation speed over the Western North Pacific. *Atmosphere* 11:93
- Zhao H, Pan J, Han G, Devlin AT, Zhang S, Hou Y (2017) Effect of a fast-moving tropical storm wash on phytoplankton in the northwestern South China sea. *J Geophys Res Oceans* 122:3404–3416
- Zhao B, Qiao F, Wang G (2008) The effects of the non-breaking surface wave-induced vertical mixing on the forecast of tropical cyclone tracks. *Chin Sci Bull* 59:3075–3084
- Zhao H, Tang D, Wang Y (2008) Comparison of phytoplankton blooms triggered by two typhoons with different intensities and translation speeds in the South China sea. *Mar Ecol Prog Ser* 365(57):65
- Zheng ZW, Ho CR, Zheng Q, Kuo NJ, Lo YT (2010) Satellite observation and model simulation of upper ocean biophysical response to super typhoon nakri. *Cont Shelf Res* 30:1450–1457
- Zhu T, Zhang DL (2006) The impact of the storm-induced SST cooling on hurricane intensity. *Adv Atmos Sci* 23:14–22

Publisher's Note

Springer Nature remains neutral with regard to jurisdictional claims in published maps and institutional affiliations.

Submit your manuscript to a SpringerOpen[®] journal and benefit from:

- Convenient online submission
- Rigorous peer review
- Open access: articles freely available online
- High visibility within the field
- Retaining the copyright to your article

Submit your next manuscript at ► [springeropen.com](https://www.springeropen.com)
